Nuclear Inst. and Methods in Physics Research, A 950 (2020) 162972

Contents lists available at ScienceDirect

Nuclear Inst. and Methods in Physics Research, A

journal homepage: www.elsevier.com/locate/nima

Measurements and FLUKA simulations of aluminium, bismuth and indium activation by stray radiation from the annihilation of low energy antiprotons

C. Ahdida [a], R. Froeschl [a], E. Iliopoulou [a], A. Infantino [a,*], S. Jensen [a,b]

[a] CERN, 1211 Geneva 23, Switzerland
[b] Department of Physics and Astronomy, Aarhus University, Denmark

ARTICLE INFO

Keywords:
Benchmark
Activation
AD
Antiproton
Monte Carlo
FLUKA

ABSTRACT

The Antiproton Decelerator at the CERN Proton Synchrotron complex provides antiprotons at a kinetic energy of 5.3 Mev to several experiments. The stray radiation from antiproton annihilations is the most important radiation field for radiation protection in the Antiproton Decelerator experimental areas.

In August 2018, aluminium, bismuth and indium samples have been exposed to the annihilation stray radiation. The resulting induced radioactivity has been measured and compared to the predictions of FLUKA Monte Carlo simulations.

The observed agreement between the FLUKA predictions and the measured values is better than a factor of 2.

1. Introduction

The CERN Antiproton Decelerator (AD) facility began operation in 1999 to serve experiments for studies of CPT invariance by precision laser and microwave spectroscopy of antihydrogen and antiprotonic helium atoms. The unique features of this facility allows accessing a series of physics experiments, which are summarized in several publications, such as [1,2].

The AD provides low-energetic antiprotons to several experiments located in the CERN AD hall. Antiprotons are created in the hadronic shower resulting from the interaction of a 26 GeV/c proton beam, extracted from the Proton Synchrotron (PS), with an iridium target. The antiprotons emerging from this shower pass through a magnetic horn where charged particles are bent by a toroidal magnetic field and focused (or defocused) in the forward direction, depending on the respective charge. A collimator located downstream the magnetic horn allows reducing the shower towards the AD hall as well as the absorbed dose received by the machine equipment. A magnetic "dog-leg", composed by a set of bending dipoles and quadrupoles, allows the application of a momentum selection of ± 3% around the momentum mean value of 3.57 GeV/c, for which the injection into the AD ring is designed [4]. Finally, the antiprotons are transferred to the AD ring, where they are decelerated to a kinetic energy of 5.3 MeV using both stochastic and electron cooling [5]. After deceleration, they are ejected to the AD experimental areas.

In the AD experimental areas, the antiprotons finally hit components resulting in their annihilation. These interactions produce stray radiation [3], which is the main radiation source of interest for radiation protection in the AD experimental areas, as it might lead to the exposure of persons and activate material.

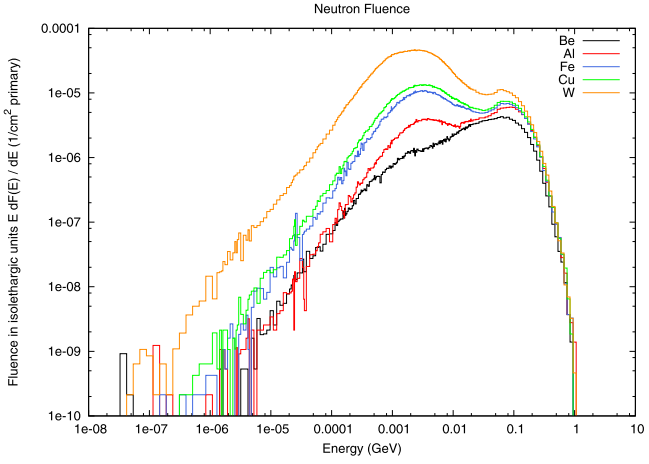

Fig. 1. Comparison of neutron fluences at 1 m distance from the antiproton annihilation point for different metals. The low energetic neutrons show a large dependency on the material while the fluence of highly energetic neutrons increases only slightly with the mass number A [3].

* Corresponding author.
E-mail address: angelo.infantino@cern.ch (A. Infantino).

https://doi.org/10.1016/j.nima.2019.162972
Received 9 July 2019; Received in revised form 20 September 2019; Accepted 1 October 2019
Available online 16 October 2019

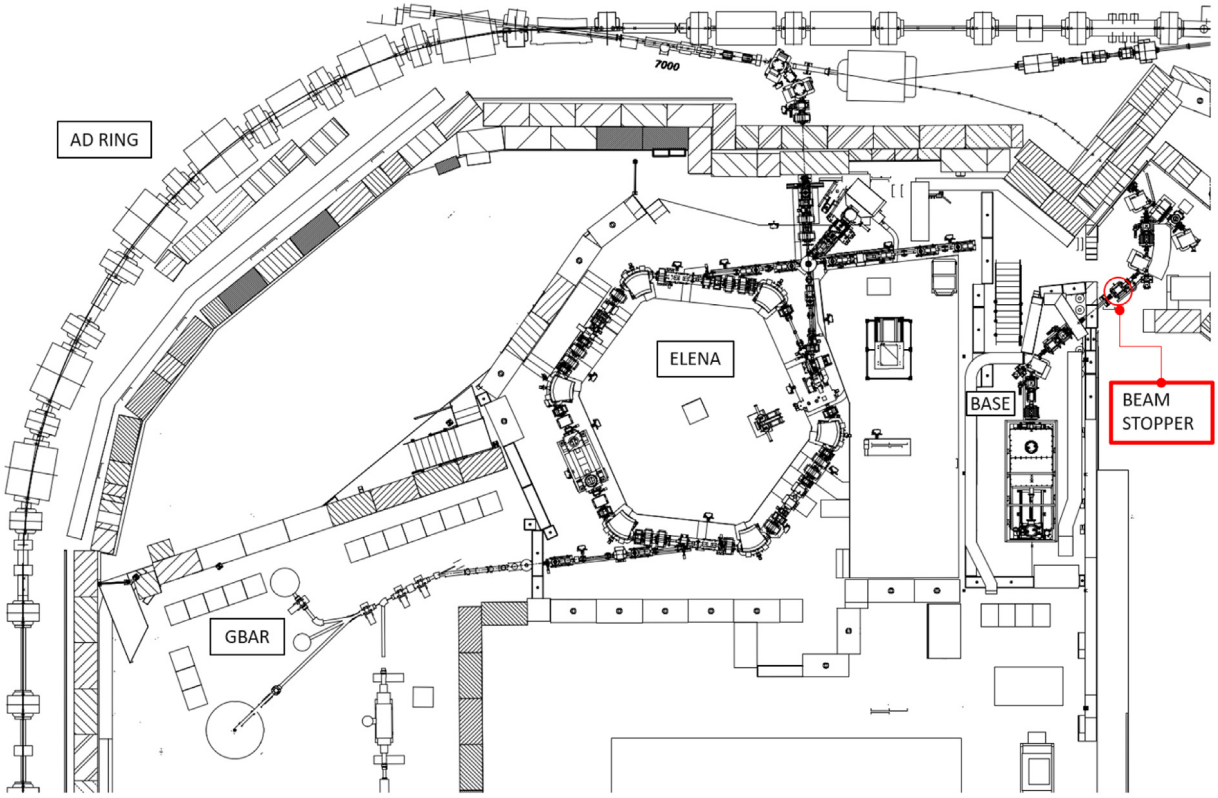

Fig. 2. Location of the beam stopper where the activation experiment has been conducted. The map shows only the area of interest of the AD hall.

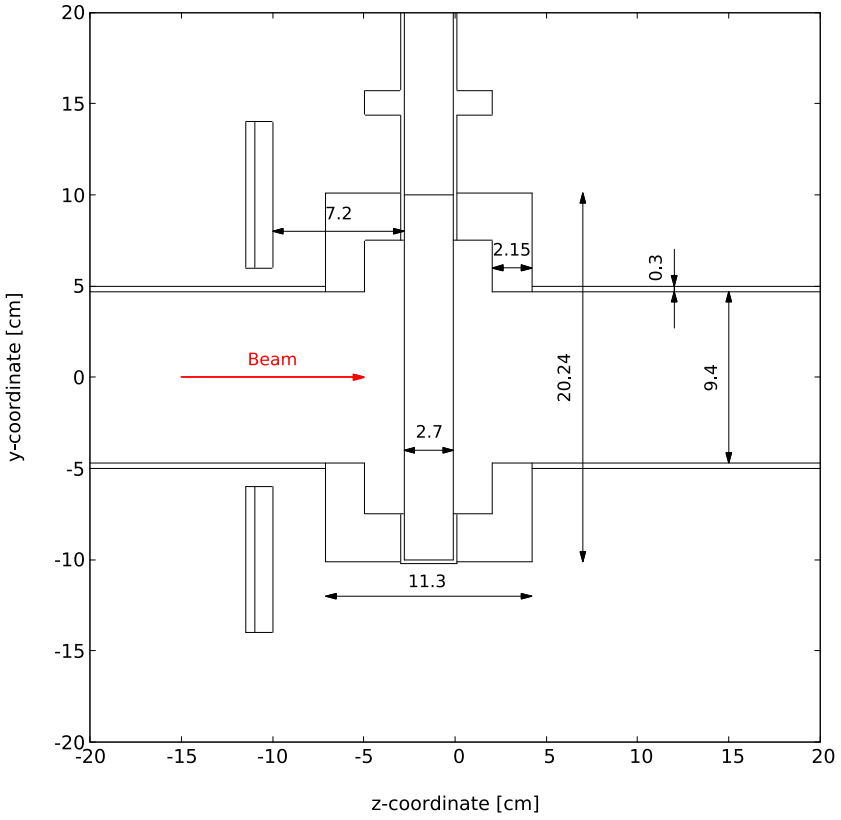

Fig. 3. Lateral view ($x = 0$) of the experimental setup. The sketch shows the main dimensions of the vacuum valve plate, the connecting flanges, the beam pipe and distance of the samples from the front face of the plate. All dimensions are reported in cm.

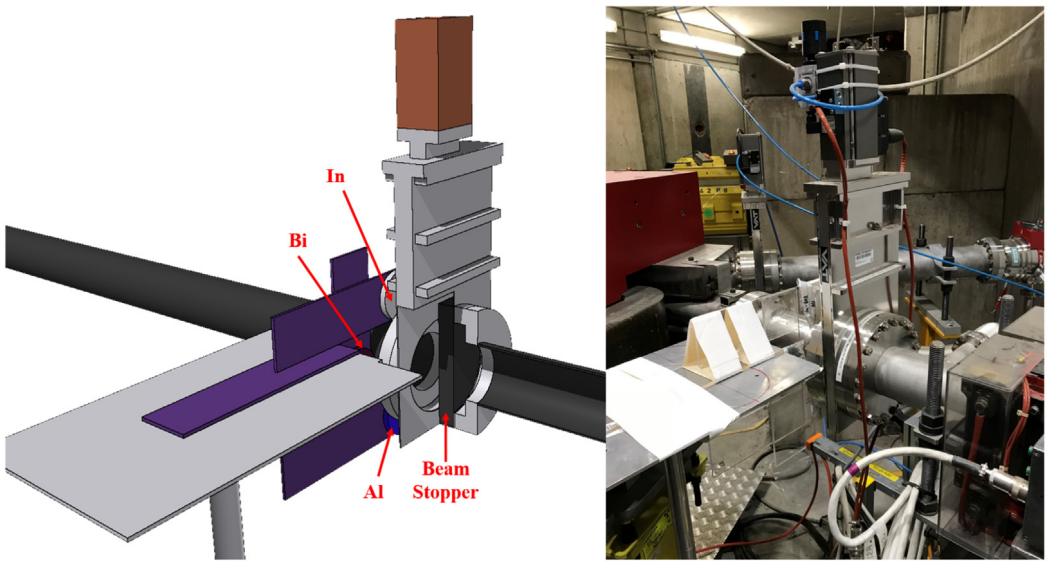

Fig. 4. FLUKA geometry (left) and photo (right) of the experimental setup. The Plexiglas holder is illustrated in purple in the FLUKA geometry.

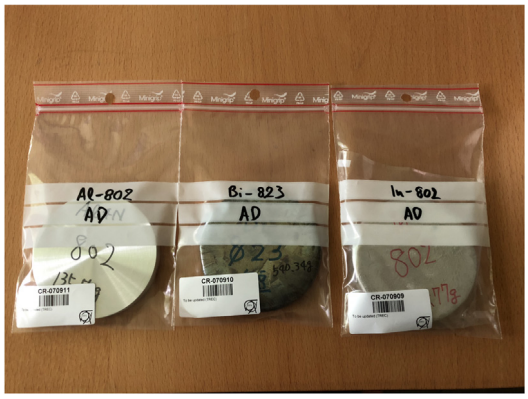

Fig. 5. Samples that have been exposed to stray radiation from antiproton annihilation.

The FLUKA Monte Carlo code [6,7] is a valuable tool used at CERN for several applications such as machine protection, radiation-to-electronics, radiation protection studies [8–10] as well as in several FLUKA benchmarking activation studies [11–14]. More specifically, FLUKA has been used already for several radiation protection studies of the AD experimental areas [3,15,16]. Nevertheless, an experimental validation of the capability of the FLUKA code to correctly reproduce the stray radiation field from antiproton annihilations in massive target nuclides was missing in literature.

As of now, stray radiation measurements of proton–antiproton annihilations, such as given in [17], have been published. The neutron fluences from the antiproton annihilation in different materials, as presented in Fig. 1, however is largely dependent on the target material. Therefore, the existing proton–antiproton annihilation data cannot be translated to massive target nuclides. So far, only the fragment multiplicity has been measured for both minimally and heavily ionizing particles for antiproton annihilations in copper, silver and gold [18].

This study aims to benchmark the description of activation due to the stray radiation from the annihilation of low-energy antiprotons by the FLUKA code via activation measurements of samples that have been exposed to this stray radiation.

Table 1
Main data of the irradiated samples and of the γ-ray spectrometry measurements at the CERN γ-ray spectrometry laboratory. All samples have been measured for 3 h. The purity of all samples is at least 99.99 mass–%.

Material	Dimensions (mm)	Mass (g)	γ-ray spectrometry detector efficiency	Start of γ-ray spectrometry measurement (date and time)
Al	80(⌀)×10	135.55	57%	13/08/18, 10:25:16 AM
Bi	80(⌀)×10	540.34	29%	13/08/18, 10:32:00 AM
In	80(⌀)×10	384.77	68%	13/08/18, 10:19:45 AM

2. Materials and methods

2.1. Samples and experimental setup

The activation experiment was performed with antiprotons being directed onto a closed vacuum valve, that acts as a beam stopper, located in the AD hall (see Fig. 2). The experiment was performed in August 2018, by using the setup depicted in Fig. 4.

Three disc samples in total, one aluminium, one bismuth and one indium sample, have been placed around the beam stopper by means of a Plexiglas support and irradiated for nearly 3 h. The relative position of the samples with respect to the front surface of the beam stopper was accurately measured. The centre of the discs was placed at 7.2 cm (aluminium and indium) and 7.7 cm (bismuth), upstream of the vacuum valve and 10 cm radially from the beam axis. After the irradiation, the samples were measured at the CERN γ-ray spectrometry laboratory, using different High-Purity Germanium (HPGe) detectors. The main data of the samples, including their dimensions and masses, the times of measurement and detector efficiencies are reported in Table 1 while the samples are shown in Fig. 5.

The vacuum valve is a series 10 model commercially available from VAT and the flange is of type CF150 with an outside diameter of 20.3 cm. The vacuum valve plate has a dimension of 20 × 20 × 2.7 cm^3 and is made out of stainless steel type 316L as it is the case for its surrounding holding structure and the vacuum pipe for the beam. The beam pipe has an inner diameter of 9.4 cm and a thickness of 0.3 cm. Laterally to the beam stopper, an aluminium table was placed onto which a Plexiglas support (0.5 cm thick) for the samples was mounted. Fig. 3 shows the main dimensions of the vacuum valve plate, the beam pipe and distance of the samples from the front face of the plate.

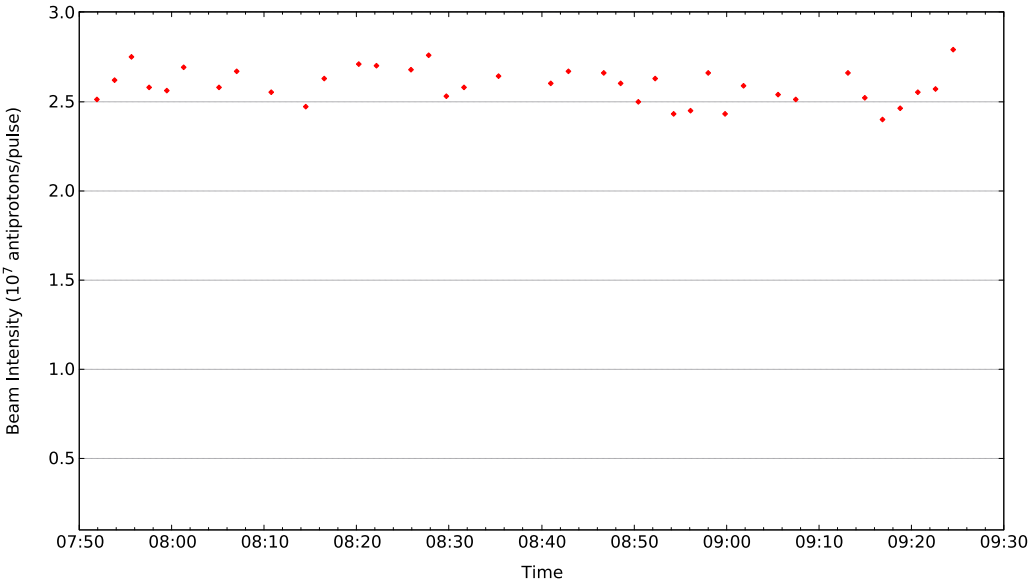

Fig. 6. Beam intensity per injection as measured by the beam current transformer during the activation experiment.

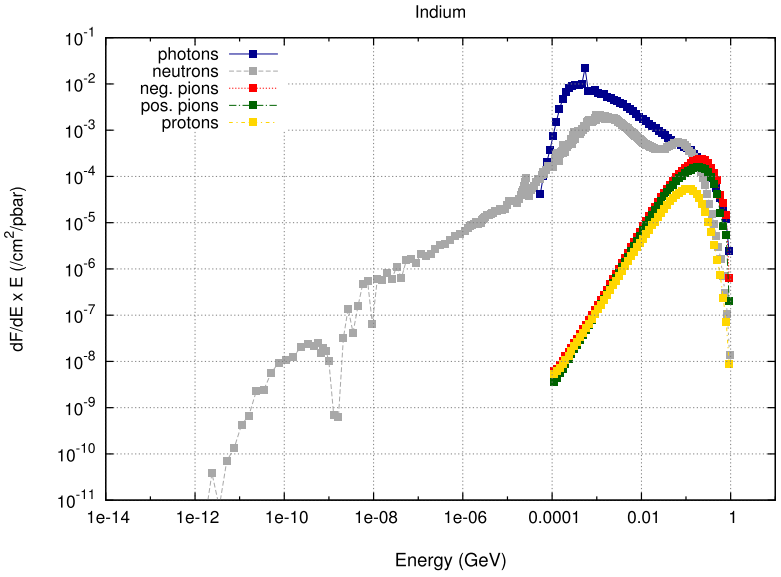

Fig. 7. Isolethargy fluence spectra of photons, neutrons, π^-, π^+ and protons in the indium sample obtained with FLUKA.

Table 2
Parameters of the antiproton beam during the activation experiment.

Kinetic energy	5.3 MeV
FWHM (horizontally)	0.12 cm
FWHM (vertically)	0.27 cm
Average antiproton intensity per pulse	2.59×10^7
Average cycle length	110 s

2.2. Facility and beam parameters

The main parameters of the antiproton beam during the activation experiment are summarized in Table 2. The beam intensity was measured with a beam current transformer placed in the AD ejection line. For the given measurement, the systematic uncertainty as given in Table 5 has been provided by the CERN beam operation group. Fig. 6 shows the beam intensity during the time of the activation experiment: the average beam intensity amounted to $2.59{\times}10^7$ antiprotons per pulse.

2.3. FLUKA simulations

FLUKA Monte Carlo simulations have been performed using the latest released version (FLUKA 2011.2x.4) available at the time of the computation. The experimental setup has been modelled in all its main components at the level of detail needed as shown in Fig. 4, including the vacuum valve, the beam pipe, the activation samples, the Plexiglas support and the table. The geometry has been created using Flair [19]. The antiproton beam has been modelled using the information provided in Table 2. The density and chemical composition of stainless steel 316L, the material where the antiproton annihilation takes place, are listed in Table 3 as they were implemented in the FLUKA simulations.

Specific transport and physics settings were used in addition to the collection of the main precision physics settings: EMF production and transport thresholds were set to 100 keV for e^+/e^- and 50 keV for γ; photonuclear interactions were explicitly enabled. A detailed description of the models and cross section data used in FLUKA can be found in [6,20].

Table 3
Chemical composition of stainless steel 316L. A density of 8.03 g/cm^3 was used in the calculations.

Element	Mass fraction (%)
Fe	65.133
Cr	17
Ni	12
Mo	2.5
Mn	2
Si	0.75
Ti	0.15
N	0.1
Nb	0.1
Cu	0.1
Co	0.05
P	0.045
C	0.03
S	0.03
Ta	0.01
B	0.002

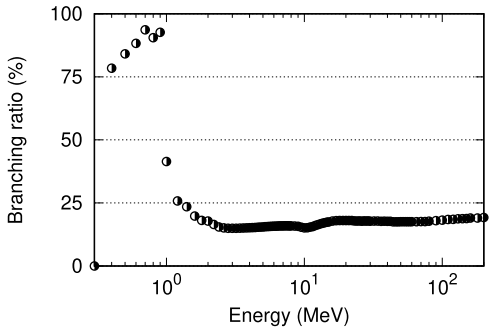

Fig. 8. Branching ratio for the ^{115}In(n,n′) ^{115m}In reaction as a function of the neutron energy from the TENDL-2017 library [22]. Uncertainty not included.

Several quantities of interest have been scored within the 3 samples, such as the radionuclide inventory, the radionuclide production yields and the differential particle fluence distributions of neutrons, π^+, π^-, photons and protons.

3. Results

Fig. 7 shows the fluence spectra of photons, neutrons, π^-, π^+ and protons in the indium activation sample volume as obtained with FLUKA. While charged particles and photons have not been transported anymore below the thresholds reported in the previous section, neutrons have been transported down to thermal energy. Moreover, the neutron spectrum of Fig. 7 shows also the effect of the strong resonance of the ^{115}In(n, γ) ^{116}In cross section, with its ~30000 barn at ca. 1.45 eV [21].

Fig. 8 illustrates the branching ratio for the ^{115}In(n,n′) ^{115m}In reaction as a function of the neutron energy from the TENDL-2017 library [22]. It shows that the branching ratio strongly depends on the neutron energy: while for neutrons in the energy range from 0.4 MeV to 0.9 MeV the branching ratio lies between 78% and 94%, it is rather flat for neutrons of higher energies with an average branching ratio of approximately 17%. To evaluate the average branching ratio relevant for the given neutron field produced in the antiproton annihilation, the branching ratio was weighted with the ^{115m}In production yield distribution obtained by weighting the neutron spectra with the production cross sections [23]. It results in a spectrum-averaged branching ratio of 18.0%. Finally, the production yield for ^{115m}In obtained from the simulation has been corrected to account for a spectrum-averaged branching ratio of 18.0% instead of the FLUKA default branching ratio of 50% [6].

The activities of the bismuth isotopes, ^{24}Na and ^{115m}In were measured in the activation samples by means of γ-ray spectrometry performed with HPGe detectors. These activities have been converted to the production yields by taking into account the corresponding irradiation profile and cool-down times. The irradiation profile has not been averaged for this calculation: the induced activity and the corresponding cool-down time have been taken into account for each injection (see Fig. 6).

The production yields predicted by FLUKA simulations and measured by γ-ray spectrometry are shown in Table 4. The resulting agreement is better than a factor of ~ 2.

An additional set of FLUKA simulations has been performed where no particles except neutrons were transported within the samples. The aim of these simulations was to compare the activation exclusively produced by neutrons with respect to the one produced by all particles. Table 4 includes also the contribution of neutrons to the total production yield assessed by FLUKA simulation. The simulations considering only the neutron contribution provide a production yield up to a factor ~ 2 lower than the simulations considering all particles. This effect is most pronounced for the bismuth isotopes.

Finally, the main contributions to the total uncertainty have been considered in the analysis, including the statistical uncertainty of the simulations, the statistical uncertainty of the γ-ray spectrometry measurements and the uncertainty on the distance between the samples and the annihilation point. The expanded uncertainty has been calculated from the quadratic propagation of all the contributions reported in Table 5.

With regard to Bi-201, the final uncertainty of ~50% mainly derives from the gamma-ray spectrometry analysis. Indeed, the irradiation conditions were not suitable for producing a relatively high, with respect to the other target radionuclides, amount of Bi-201. Therefore, the acquisition time may have not been long enough to reduce the statistical uncertainty associated to the measurement.

4. Conclusions

The CERN Antiproton Decelerator (AD) provides low-energetic antiprotons to several experiments where the antiprotons ultimately annihilate. These interactions produce a stray radiation field, which is the main radiation source of interest for radiation protection in this facility, as it might lead to the exposure of persons and activates material.

The purpose of this study is to benchmark the description of activation due to the stray radiation from the annihilation of low-energy antiprotons by the FLUKA code via activation measurements of samples. Three disc samples in total have been exposed to this stray radiation in August 2018 by directing antiprotons in the AD experimental area onto a closed vacuum valve, that acts as a beam stopper, made of stainless steel type 316L for nearly 3 h.

The production yields of different radionuclides have been assessed from the activities of the irradiated samples measured by γ-ray spectrometry and compared to the estimated production yields calculated by means of FLUKA Monte Carlo simulations. The resulting agreement is better than a factor of ~ 2, with the largest deviation occurring for ^{24}Na.

This agreement demonstrates that FLUKA is a very suitable tool for the description of activation due to the stray radiation from the annihilation of low-energy antiprotons.

The activation of the samples is a two-folded process consisting of the production of the stray radiation followed by the subsequent interaction of the stray radiation with the samples. Similar activation experiments [10–14] have also typically shown agreements between FLUKA Monte Carlo simulations and measurements of a factor of ~ 2. Having therefore gained confidence in the respective activation cross-sections, it is considered reasonable to infer that FLUKA simulates the production of the stray radiation due to the annihilation of low-energy antiprotons quite accurately.

Table 4
Comparison of production yields predicted by FLUKA simulation and measured by γ-ray spectrometry.

Material	Radionuclide	Prediction (FLUKA)		Measured yield from	Ratio
		Yield [atoms/$\bar{p}$-annihi.]	Neutron contribution	γ-spect. analysis [atoms/$\bar{p}$-annihi.]	Predicted/ Measured
Al	Na-24	1.86e−04 ± 1.5%	79%	3.24e−04 ± 15%	0.57 ± 16%
Bi	Bi-201	1.29e−04 ± 1.5%	50%	9.50e−05 ± 51%	1.36 ± 51%
	Bi-202	1.60e−04 ± 1.5%	58%	1.31e−04 ± 25%	1.23 ± 25%
	Bi-204	3.29e−04 ± 1.5%	68%	3.19e−04 ± 19%	1.03 ± 19%
In	In-115m	1.74e−03 ± 1.4%	87%	1.80e−03 ± 15%	0.97 ± 15%

Table 5
Relative FLUKA simulation and measurement uncertainties. Total relative uncertainties have been calculated as a quadratic sum of the individual relative uncertainties.

	Source of uncertainty	Uncertainty (%)				
		In-115m	Na-24	Bi-201	Bi-202	Bi-204
Simulation	Statistical	<1	0.4	0.5	0.6	0.4
	Sample mass and dimension	<1	<1	<1	<1	<1
	SS316L density and composition	<1	<1	<1	<1	<1
Measurement	Gamma Spectrometry	9.5	10.4	50.2	22.7	15.8
	Beam intensity (calibration)	5	5	5	5	5
	Beam intensity (statistical)	<1	<1	<1	<1	<1
	Beam profile	<1	<1	<1	<1	<1
	Distance from the impact point	10.2	10.2	9.6	9.6	9.6
Uncertainty FLUKA/Measurement		**15**	**16**	**51**	**25**	**19**

Acknowledgements

We would like to show our gratitude to T. Eriksson, L. Ponce and L. Bojtar from the AD beam operation section for providing beam time and the required beam tuning. We are thankful to T. Sanami (KEK, Japan) and N. Nakao (Shimizu Corporation, Japan) for providing the activation samples used in this work. We are also grateful to our colleagues from the CERN γ-ray spectrometry laboratory for their support.

References

[1] M. Hori, J. Walz, Physics at CERN's antiproton decelerator, Progr. Part. Nucl. Phys. 72 (2013) 206–253.
[2] W. Oelert, The ELENA project at CERN, Acta Phys. Pol. B 46 (2015) 181–190.
[3] R. Froeschl, S. Lohmann, Radiation fields due to anti-proton annihilation, prompt dose rates and induced activity in the AD experimental areas, Tech. Rep. CERN–RP–2013–084–REPORTS–TN, 2013, EDMS1312195.
[4] M. Calviani, E. Nowak, FLUKA implementation and preliminary studies of the AD-target area, AD: Anti proton decelerator. CERN-ATS-Note-2012-069 TECH, 2012, http://cds.cern.ch/record/1476719.
[5] T. Eriksson, AD: low-energy antiproton production at CERN, Hyperfine Interact. 194 (2009) 123–128.
[6] A. Fassò, A. Ferrari, J. Ranft, P.R. Sala, FLUKA: a multi-particle transport code, Tech. Rep. CERN-2005-10, 2005, INFN/TC-05/11, SLAC-R-773.
[7] T.T. Bohlen, F. Cerutti, M.P.W. Chin, A. Fassò, A. Ferrari, P.G. Ortega, A. Mairani, P.R. Sala, G. Smirnov, V. Vlachoudis, The FLUKA code: developments and challenges for high energy and medical applications, Nucl. Data Sheets 120 (2014) 212–214.
[8] E. Skordis, R. Bruce, F. Cerutti, A. Ferrari, P.G. Ortega, P.D. Hermes, A. Lechner, A. Mereghetti, S. Redaelli, V. Vlachoudis, Impact of beam losses in the LHC collimation regions, in: 6th International Particle Accelerator Conference IPAC2015, Richmond, VA, USA, 2015, pp. 2116–2119.
[9] A. Infantino, C. Cangialosi, M. Krawina, M. Brucoli, M. Brugger, J.P. De Carvalho Saraiva, S. Danzeca, Dose gradient assessment at the new CERN CHARM irradiation facility, Radiat. Phys. Chem. 155 (2019) 225–232.
[10] E. Iliopoulou, P. Bamidis, M. Brugger, R. Froeschl, A. Infantino, T. Kajimoto, N. Nakao, S. Roesler, T. Sanami, A. Siountas, Measurements and FLUKA simulations of bismuth and aluminium activation at the CERN Shielding Benchmark Facility (CSBF), Nucl. Instrum. Methods Phys. Res. A 885 (2018) 79–85.
[11] N. Nakao, et al., Measurement and calculation of high-energy neutron spectra behind shielding at the CERF 120 GeV/c hadron beam facility, Nucl. Instrum. Methods Phys. Res. B 266 (2008) 93–106.
[12] E. Iliopoulou, et al., Measurements and FLUKA simulations of bismuth, aluminium and indium activation at the CERN Shielding Benchmark Facility (CSBF), J. Phys.: Conf. Ser. 1046 (2018) 012004.
[13] E. Iliopoulou, Commissioning, characterization and exploitation of the CERN Shielding Benchmark Facility (CSBF), Aristotle University of Thessaloniki, Greece, 2018, CERN-THESIS-2018-171.
[14] E. Iliopoulou, et al., Measurements and FLUKA simulations of bismuth, aluminium, indium and carbon activation at the upgraded CERN shielding benchmark facility (CSBF), Presentation given at the SATIF 14, Gyeongju, South Korea, 2018.
[15] V. Chohan, et al., Extra Low ENergy Antiproton (ELENA) ring and its transfer lines: design report, CERN Yellow Reports: Monographs, CERN, Geneva, 2014.
[16] C. Theis, R. Froeschl, H. Vincke, Activation zoning of the experimental areas of the CERN anti-proton decelerator using ActiWiz 3, Presentation given at the 14th Workshop on Shielding Aspects of Accelerators, Targets, and Irradiation Facilities (SATIF-14), Gyeongju, Korea, 2018.
[17] C. Amsler, Proton-antiproton annihilation and meson spectroscopy with the crystal barrel, Rev. Modern Phys. 70 (1998) 1293–1339, http://dx.doi.org/10.1103/RevModPhys.70.1293.
[18] S. Aghion, et al., Measurement of antiproton annihilation on Cu, Ag and Au with emulsion films, J. Instrum. 12 (04) (2017) http://dx.doi.org/10.1088/1748-0221/12/04/p04021, P04021–P04021.
[19] V. Vlachoudis, FLAIR: a powerful but user friendly graphical interface for FLUKA, in: Proc. Int. Conf. on Mathematics, Computational Methods & Reactor Physics (M&C2009), Saratoga Springs, New York, 2009.
[20] G. Battistoni, T. Boehlen, F. Cerutti, P.W. Chin, L.S. Esposito, A. Fass, A. Ferrari, A. Lechner, A. Empl, A. Mairani, A. Mereghetti, P. Garcia Ortega, J. Ranft, S. Roesler, P.R. Sala, V. Vlachoudis, G. Smirnov, Overview of the FLUKA code, Ann. Nucl. Energy 82 (2015) 10–18.
[21] International Atomic Energy Agency (IAEA), Evaluated Nuclear Data File (ENDF). Database Version of 2018-12-20, https://www-nds.iaea.org/exfor/endf.htm. (Accessed 25 April 2019).
[22] A.J. Koning, D. Rochman, Modern nuclear data evaluation with the TALYS code system, Nucl. Data Sheets 113 (2012) 2841.
[23] F. Maekawa, et al., Production of a dosimetry cross section set up to 50 MeV, in: Proc. 10th International Symposium on Reactor Dosimetry, Sep. 12–17, 1999, Osaka, Japan, American Society for Testing and Materials, 2001, p. 417.